Original Research

AID assists DNMT1 to attenuate BCL6 expression through DNA methylation in diffuse large B-cell lymphoma cell lines ⊙ CrossMark

Junna Jiao [a,b,1]; Zhuangwei Lv [a,b,1]; Ping Zhang [a,b,1]; Yang Wang [a,b]; Meng Yuan [a,b]; Xiaozhuo Yu [a,b]; Woodvine Otieno Odhiambo [a,b]; Mingzhe Zheng [a,b]; Hua Zhang [a,b]; Yunfeng Ma [a,b]; Yanhong Ji [a,b,*]

[a] Department of Pathogenic Biology and Immunology, School of Basic Medical Sciences, Xi'an Jiaotong University Health Science Centre, Xi'an, Shaanxi, China; [b] Key Laboratory of Environment and Genes Related to Diseases (Xi'an Jiaotong University), Ministry of Education of China, Xi'an, Shaanxi, China

Abstract

The *BCL6* proto-oncogene encodes a transcriptional repressor, which is required for germinal centers (GCs) formation and lymphomagenesis. Previous studies have been reported that the constitutive expression of *BCL6* leads to diffuse large B cell lymphoma (DLBCL) through activation-induced cytidine deaminase (AID) mediated chromosomal translocations and mutations. However, other DLBCLs (45%) without structural variants were characterized by abnormally high level of *BCL6* expression through an unknown mechanism. Herein, we report that deficiency in AID or methyltransferase 1 (DNMT1) triggers high level of *BCL6* expression. AID-DNMT1 complex binds to −0.4 kb −0 kb region of *BCL6* promoter and contributes to generate *BCL6* methylation which results in inhibition of BCL6 expression. The proteasome pathway inhibitor MG132 induces accumulation of AID and DNMT1, causes decreased *BCL6* expression, and leads to cell apoptosis and tumor growth inhibition in DLBCL cell xenograft mice. These findings propose mechanistic insight into an alternative cofactor role of AID in assisting DNMT1 to maintain *BCL6* methylation, thus suppress *BCL6* transcription in DLBCL. This novel mechanism will provide a new drug selection in the therapeutic approach to DLBCL in the future.

Neoplasia (2020) 22 142–153

Introduction

The affinity maturation in humoral response is critical for effective host defense against microbial infections and tumors. The process depends on two B lymphocyte differentiation mechanisms: Ig somatic hypermutation (SHM) and class switch DNA recombination (CSR) [1–4]. Antigens stimulate naive B cells to develop to be germinal center B cells (GCBs), which leads to upregulation of activation-induced cytidine deaminase (AID) expression [5,6]. The functions of AID could be summarized as following. Firstly, the deamination of AID converts cytosine in WGCW and WRC (W = A/T, R = A/G) motifs to uracil and produces U:G mismatch, then the error-prone repair cascade replaces the uracil in U:G mismatch to cause point mutations and double strand breaks (DSBs) for SHM and CSR, respectively [7–9]. Secondly, the deaminated 5mC by AID is recognized

as a T and the generated T:G mismatch is finally corrected by C:G in error-prone repair pathway, which would implicate that AID involved DNA demethylation beyond DNA editing [10–14]. Third, AID prone to interact with some gene transcription regulatory factors (such as RAN PolII, Spt5), suggesting a alternative cofactor role of AID in regulating gene expression [15–17]. Thus, studies on AID are of considerable interest not only because of its central role in the generation of effective humoral immunity, but also because of its function in DNA methylation diversity or as a cofactor in GCBs, which potentiates AID mediated gene expression by epigenetic modifications or alternative cofactor role in B cell lymphoma.

AID's function is not restricted to Ig loci, about 25% of highly expressed non-Ig genes in GCBs are mutated by AID because AID targeted hotspot motif lacks strict specificity [18,19]. Among these non-Ig genes, the proto-oncogene *BCL6* is preferred to be deaminated by AID. BCL6 is a master regulator of the GC response to transcriptionally repress DNA

damage response, cell cycle arrest and B cell maturation [20,21]. In the development of GCBs, BCL6 positively regulates *AID* expression to mediate SHM in centroblasts formed dark zone or CSR in centrocytes formed light zone [20,21]. The accumulation of DNA lesions originated from high level of AID indirectly involves in BCL6 degradation, which is a feedback to decrease *AID* expression [22–24]. As a consequence, B cells with the highest affinity antibodies for antigens exit light zone of GC and mature to be plasma cells or memory B cells [25]. Genomic aberrations of *BCL6* or alterations of genes that modulate *BCL6* expression during the GC reaction lead to sustained BCL6 activation, which promotes the development of GC-derived lymphomas [26]. *BCL6* overexpression is achieved through AID induced translocations in the first intron (∼40%) or mutations of its promoter (∼15%) in DLBCL patients [27]. However, in other DLBCLs (∼45%) without *BCL6* mutations or translocations [27], whether AID involved in modulating *BCL6* expression is yet to be confirmed.

Here, we used the AID-deficient DLBCL cells to identify that AID and DNMT1 formed a complex to maintain the methylation of *BCL6* promoter, thus negatively regulated *BCL6* transcription by binding to its −0.4 kb −0 kb promoter region. Moreover, the proteasome inhibitor MG132 blocked degradation of AID and DNMT1, and resulted in accumulation of AID and DNMT1, manifesting apparent cell apoptosis and tumor growth inhibition. Our results provide a mechanistic insight into the inhibition function of AID to subcutaneous DLBCL cell xenograft tumor, and identify undeveloped effect of MG132 in the repression of *BCL6* expression and DLBCL treatment through inhibiting AID and DNMT1 degradation.

Materials and methods

Constructs and cells

The pCas9-AID and pCas9-DNMT1 recombinant transgenes with gRNAs for *AID* and *DNMT1* were constructed by ligating gRNA for AICDA or DNMT1 to pL-CRISPR.EFS.PAC plasmids, respectively. The sequences of gRNAs for AICDA or DNMT1 were listed in the Supplementary Table S1. The gRNA sequences were commercially confirmed (Sunny). pWPI-AID-GFP and pWPI-BCL6-GFP lentivirus constructs were ligated AID and BCL6 cDNA to pWPI-GFP plasmids, respectively. The sequences of primers for amplifying AID and *BCL6* cDNA as following: *AID*_F (5′-CTGGACACCACTATGGACAGCCTCTTGATG-3′), *AID*_R (5′-CATTCCTG

GAAGTTGCTATTAAAGTCCC-3′); *BCL6*_F (5′-GGGTTTAAA CATGGCCTCG

-CCGGCTGACAG-3′) and *BCL6*_R (5′-GGGTTTAAACTCAGCA GGCTTTGG

-GGAGCT-3′).

The SU-DHL-4, OCI-LY10, OCI-LY19 and OCI-LY7 DLBCL cell lines were purchased from BeNa Culture Collection (BeNa, #BNCC340176, #BNCC337742, #BNCC338225, #BNCC340174). Cells were cultured at 37 °C with 5% CO_2 in IMDM (Hyclone) supplemented with 10% fetal bovine serum (FBS) (Sigma), non-essential amino acids, and penicillin–streptomycin (1%), and β-mercaptoethanol (50 μM). 293 T cells were stored in our laboratory and cultured in DMEM (Hyclone) supplemented with 10% FBS, non-essential amino acids, and penicillin–streptomycin at 37 ☒ with 5% CO_2. In nutrition deficiency treatment, cells were treated by culturing in FBS free IMDM (Hyclone) supplemented with 1% penicillin–streptomycin. To generate stable DLBCL cell lines with integrated pCas9-AID and pCas9-DNMT1 transgenes, the plasmids pCas9-AID and pCas9-DNMT1 were transfected into 293 T cells being seeded 24 hours before transfection at a density of 1×10^6 cells per 5-cm plate, cotransfected with the ΔR9 and pVSVG helper plasmids using the X-tremeGENE HP DNA transfection

reagent (Roche, #06366236001). Supernatants were collected 72 hours after transfection. 1×10^6 DLBCL cells were infected with a freshly prepared *AID* or *DNMT1* knock out lentivirus by performing a 1000 g spin at room temperature for 90 minutes in the presence of 10 μg/ml polybrene. Stably integrated DLBCL cells were selected by puromycin (0.4 μg/ml) for 5 days. To generate *AID* or *BCL6* over-expressing DLBCL cell lines, 1×10^6 DLBCL cells were infected with *AID* or *BCL6* expressing lentivirus for 5 days and then were sorted by BD AriaIII.

Cells were treated with 5-Azacytidine (10 μM) (Selleckchem, #S1782) for 24 h. Combined treatment with MG-132 (10 μM) (Selleckchem, #S2619) was done for another 8 h following pre-treatment with 5-Azacytidine (10 μM) for 16 h. Control cells were only treated with a solvent (DMSO).

RNA extraction and quantitative RT-PCR

Total RNA of DLBCL cell pellets was extracted with TRIzol (Invitrogen, #15596026) according to the manufacturer's instructions. cDNA was then synthesized with PrimeScript™ RT reagent Kit (TaKaRa, #RR037A), according to the manufacturer's protocol. Quantitative PCR was performed with real-time PCR using Mx3000P (Agilent Technologies). Primers were listed in Supplementary Table S2. The relative mRNA level of genes were calculated according to the formula $2^{-\triangle\triangle Ct}$ using β-actin as an internal control.

Genomic DNA isolation and bisulfite sequencing

Genomic DNA was extracted from 1 to 5×10^6 cells using the Genomic DNA Extraction Kit (TaKaRa, #D824A) according to the manufacturer's protocol. The genomic DNA was converted by bisulfite treatment using the EZ DNA Methylation-Gold Kit (Zymo Research, #D5006) and amplified by PCR with the EpiTaq™ HS Kit (TaKaRa, #R110A). The CpG island containing CpG sites in BCL6 promoter were predicted according to the website for methylation primer designing (http://www. urogene.org/methprimer/). The primer sequences used for analyzing the methylation status of 4CpG sites and 17 CpG sites in *BCL6* promoter regions were *BCL6*-4 meth_F (GTTTTGGTTATGAGAGTTTTT-TAAG) and *BCL6*-4 meth_R (AAAATACATTACCAACAACATT TTC); *BCL6*-17 meth_F (GTTATTTAGAAGGATAGGGGAAGG) and *BCL6*-17 meth_R (TCTAAAAACTATCTAACCCCAAACC). Amplicons were visualized on a 1.0% agarose gel. They were then excised, purified with the OMEGA Gel Extraction Kit (OMEGA, #D2500-01), and cloned into the pMD® 18-T vector (TaKaRa, #D103A). DNA containing amplicon inserts were identified by digestion with Xbal and SalI restriction enzymes and sequenced commercially (Sunny). Sequence analysis showed a bisulfite-modification efficiency of 99–100%.

The −0.92 kb to 0 kb of *BCL6* gene was amplified from genomic DNA and cloned into the pMD® 18-T vector (TaKaRa, #D103A). After confirmation by Xbal and SalI restriction enzymes, the vector with the target fragments were commercially sequenced (Sunny). The primers were *BCL6* TSS_F (TTGTCCCAAGTCACACTGGA) and *BCL6* TSS _R (AGTGCAAATCATAGCTGGGG).

The fragments containing the first intron of *BCL6* gene were amplified from genomic DNA by long-range PCR according to the manufacturer's protocol of TaKaRa LA PCR™ Kit Ver.2.1 (TaKaRa, #RR013A). The sequences of primers were *BCL6* intron 1_F (ATTCTCCATGTCTGCC CCAA) and *BCL6* intron 1_R (ACTCGCCTCTCTAACCCTAC).

Flow cytometry and antibodies

To measure the proliferation and apoptosis ability of DLBCL cells, cells were prepared and stained according to standard procedures.

Measuring the ability of cells to proliferate involved the use of anti-CFSE (carboxyfluorescein succinimidyl ester) (BD eBioscience, #C34554) to stain the cells in advance for 6 hours. The cells were then washed twice with 1 × PBS at 4 °C and analyzed by flow cytometry. Nutrition deficiency was performed to measure apoptosis. Cells were collected and washed twice with 1 × PBS at 4 °C, incubated with anti-Annexin V and anti-7-ADD (BD eBioscience, #559763) for 15 minutes at room temperature. Finally, the cells were resuspended in flow cytometry buffer and analyzed by flow cytometry. All data were collected using a CytoFLEX Flow Cytometer (Beckman Coulter).

Immunoblot analysis

Cell pellet was lysed in RIPA buffer [50 mm Tris-HCl (pH 8.0), 0.15 m NaCl, 1% Triton X-100, 0.5% NaDoc, 0.1% SDS, 1 mm EDTA, 1 mm EGTA, 1 mm PMSF (Amersco) and 1 μg/ml Pepstatin A (Sigma) protease inhibitors]. The cells were then sonicated using BioruptorTMUCD-200 (Diagenode) for 15 min at a low speed. Cell lysates were centrifuged for 20 min at 15 000g at 4 °C, and the protein supernatant was collected. Protein samples were loaded on a 10% (w/v) Tris-HCl SDS-PAGE gels for electrophoresis, transferred to PVDF membrane (Millipore), blotted, and then probed with anti-AID (CST, #4959), anti-BCL6 (Abcam, #ab33901), anti-DNMT1 (Abcam, #ab13537), anti-DNMT3A (Abcam, #ab2850), anti-DNMT3B (Abcam, #b2850), anti-Caspase 3 (Abcam, #ab13586) antibodies. Anti-GAPDH (Abcam, #ab9485) was used as a loading control. The signal was further detected using the secondary antibody of goat anti-Rabbit, goat anti-Rat, goat anti-Mouse IgG conjugated with horseradish peroxidase (Thermo Fisher). Band signal was visualized by Immobilon™ Western Chemiluminescent HRP substrate (Millipore). Integrating optical density was analyzed using gel-pro analyzer software (Media Cybernetics) and ratios of bands were all referenced to the loading control.

Immunoprecipitation

Briefly, Total protein was extracted as described in the part of immunoblot analysis. After pre-clearing the chromatin with Dynabeads Protein G beads (2 ×) (Invitrogen, #10003D), set a part of the aliquot aside as the input sample. Proteins from 5 × 10^6 cells were then incubated with 5 μg specific antibody or normal goat IgG (Santa Cruz, #sc2346) for overnight at 4⊠. Anti-AID (Abcam, #ab59361), anti-DNMT1 (Abcam, #ab13537), immune complexes were pulled down through incubation with Dynabeads Protein G beads (2 ×) (Invitrogen, #10003D) for 3 hours. The beads were washed at 4 °C for ten times with RIPA buffer containing different concentration of NaCl. The pulldown proteins were denatured at 100 °C, and loaded on SDS-PAGE gels to perform immunoblot.

Chromatin immunoprecipitation

The chromatin immunoprecipitation (ChIP) was carried out according to the methods reported by Ji Y [28,29]. Briefly, 30 × 10^6 cells were cross-linked with 1% HCHO (Sigma) for 15 min at room temperature, and the reaction was terminated with 0.125 m glycine. The precipitate was washed, resuspended in RIPA buffer and sonicated to fragment DNA of 0.3–0.5 kb. After pre-clearing the chromatin with Dynabeads Protein G beads (2 ×) (Invitrogen, #10003D), about one tenth of the aliquot was stored up as the input sample. The remnants were incubated with 5 μg specific antibody or normal IgG overnight at 4 °C. Immune complexes were pulled down with Dynabeads Protein G beads (2 ×) (Invitrogen, #10003D). After reversal of cross-links and purification of the DNA, qPCR was performed using SYBR Premix Ex Taq™ II (TaKaRa,

#DRR081A) with Mx3000 thermocycler (Agilent Technologies). The primer sequences used for qPCR were ChIP-BCL6_F (CCTTCGCTGTAG-CAAAGCTC) and ChIP-BCL6_R (AACCTCTCGCTCCCTTTTGT). Input samples were diluted so that each IP and input sample would give approximately equal qPCR signals. Using standard curves generated for each region analyzed in each experiment, the amount of DNA obtained from immunoprecipitates and the input chromatin was calculated. ChIP-qPCR signals were expressed according to the following equation: (IP/Inputcorr)/positive control = (((IPspecific antibody − IPIgG)/ Input) × 1000)/positive control. ChIP experiments were performed with antibodies for anti-AID (Abcam, #ab59361), anti-DNMT1 (Abcam, #ab13537) and normal goat IgG (Santa Cruz, #sc2346).

Construction of luciferase plasmids and transient reporter assay

The fragments of promoter (p) and the sub-regions 1–4 (p1, p2, p3 and p4) of BCL6 gene were amplified by PCR from genomic DNA. Primers used were listed in Supplementary Table S3. The amplified fragments were digested with MluI and XhoI and were cloned into the pGL3-basic vector upstream of the firefly luciferase–encoding region. The constructed vector sequences were commercially confirmed (Sunny, China). SU-DHL-4, OCI-LY10 and OCI-LY19 cells were transiently transfected by equimolar amounts of reporter constructs with BCL6 promoter segments and the pGL3-basic vectors together with the X-tremeGENE HP DNA transfection reagent (Roche, #06366236001). Cells were cultured for 72 hours prior to collection. Luciferase activity was measured by the Luciferase Assay kit (Promega, #E1500) with an EnVision 2103 Multilabel Reader (PerkinElmer). Luciferase activity was presented as the `fold change' relative to that obtained with pGL3-basic.

In vivo tumor cell engraftment and treatment of mice

NOD/SCID (Non-obese diabetic/severe combined immunodeficiency) mice were maintained in specific pathogen-free facilities at the Xi'an Jiaotong University Laboratory Animal Center. A murine model of human DLBCL was established by subcutaneous injection of 2 × 10^7 DLBCL cells into the right flank of NOD/SCID mice. The tumor growth was monitored by measuring tumor size in two orthogonal dimensions. Tumor volume was calculated using the formula ø(long dimension)(short dimension)^2. MG132 (10 μM) therapy was initiated when the average tumor volume reached 80 mm^3–100 mm^3. The DLBCL tumor-bearing NOD/SCID mice were divided into control group (n = 5) and treatment group (n = 5). The mice in treatment group were intraperitoneally injected with MG132 (50 mg/kg), while the mice in control group was received an intraperitoneal injection with an equal volume of solvent (4% DMSO + 30% PEG300 + 20% Propylene glycol + ddH$_2$O). Tumor volume was continuously monitored twice every weekly (on Mondays and Wednesdays). All of the mice were euthanized 24 days post MG132 therapy. The tumors in the control and treatment groups were excised and weighed. All animal procedures were approved by the Institutional Animal Care and Use Committee of Xi'an Jiaotong University.

Statistical analysis

Unpaired t-test and ANOVA multiple tests were performed with GraphPad Prism 6.0 (GraphPad Software, LaJolla, CA, USA). Data were considered statistically significant if p values were less than 0.05, as indicated.

Results

AID loss impairs DLBCL cell apoptosis by elevating BCL6 level

To explore the action of AID in DLBCL cells without BCL6 translocations, genomic DNA derived from SU-DHL-4, OCI-LY10 and OCI-LY19 DLBCL cell lines were amplified for 12.7 kb `major breakpoint region' spanning *BCL6* intron 1 by using long-range PCR, respectively [30] (Fig. S1A). SU-DHL-4 cells were used as a negative control because previous studies have been reported that they were lack of rearrangement for *BCL6* locus, while OCI-LY7 cells carrying *BCL6* rearrangement were taken as positive control [31]. The relative density of the PCR products for *BCL6* intron 1 showed insignificant difference in OCI-LY10 and OCI-LY19 compared to that in SU-DHL-4, indicating the selected DLBCL cells lacked BCL6 translocations (Fig. S1B). To further exclude the absence of rearrangement in both alleles of *BCL6* gene, semi-quantitative PCR for amplifying *BCL6* intron 1 products was performed to SU-DHL-4, OCI-LY10 and OCI-LY19 cells (Fig. S1C). We observed that the relative density of PCR fragments derived from OCI-LY10 and OCI-LY19 cells were equal to that from SU-DHL-4 cells (Fig. S1D). These results demonstrate that the *BCL6* translocations are absent in the three selected SU-DHL-4, OCI-LY10 and OCI-LY19 DLBCL cell lines.

The DLBCL cells were transduced using CRISPR/Cas9 with gRNAs for *AID* to generate *AID* knockout SU-DHL-4 (4AIDKO), OCI-LY10 (10AIDKO) and OCI-LY19 (19AIDKO) cell lines, respectively (Fig. S2A). The levels of mRNA and protein for AID were significantly depleted in the three AIDKO DLBCL cells compared to their wild-type (WT) counterparts (Fig. 1A to D). To determine whether AID loss had an impact on cellular function, apoptosis of AIDKO DLBCL cells were rigorously examined using Annexin V staining in absence of nutrition. The three AIDKO cells presented approximately 30% less of Annexin V^+ populations compared to that derived from WT ones ($p < 0.001$) (Fig. 1E), indicating reduced apoptosis of DLBCL cells after AID deficiency. The cells labeled with CFSE were monitored and dye dilution was tracked by flow cytometry, the collected data showed that the cell division rates of 4AIDKO, 10AIDKO and 19AIDKO cells were faster than those of WT cells (Fig. S2B). In addition, the transcripts of pro-apoptosis genes (*FAS*, *BIMEI*, *BMF*, *BAD* and *BAX*) obviously dropped in AIDKO cells (all $p < 0.05$) (Fig. S2C). Meanwhile, the transcription levels of anti-apoptotic genes (*BCL2*, *A1*, *BCLW*, *CLAP1*, *CFLIP*, *MCL1*) apparently increased in AIDKO cells (all $p < 0.05$) (Fig. S2D).
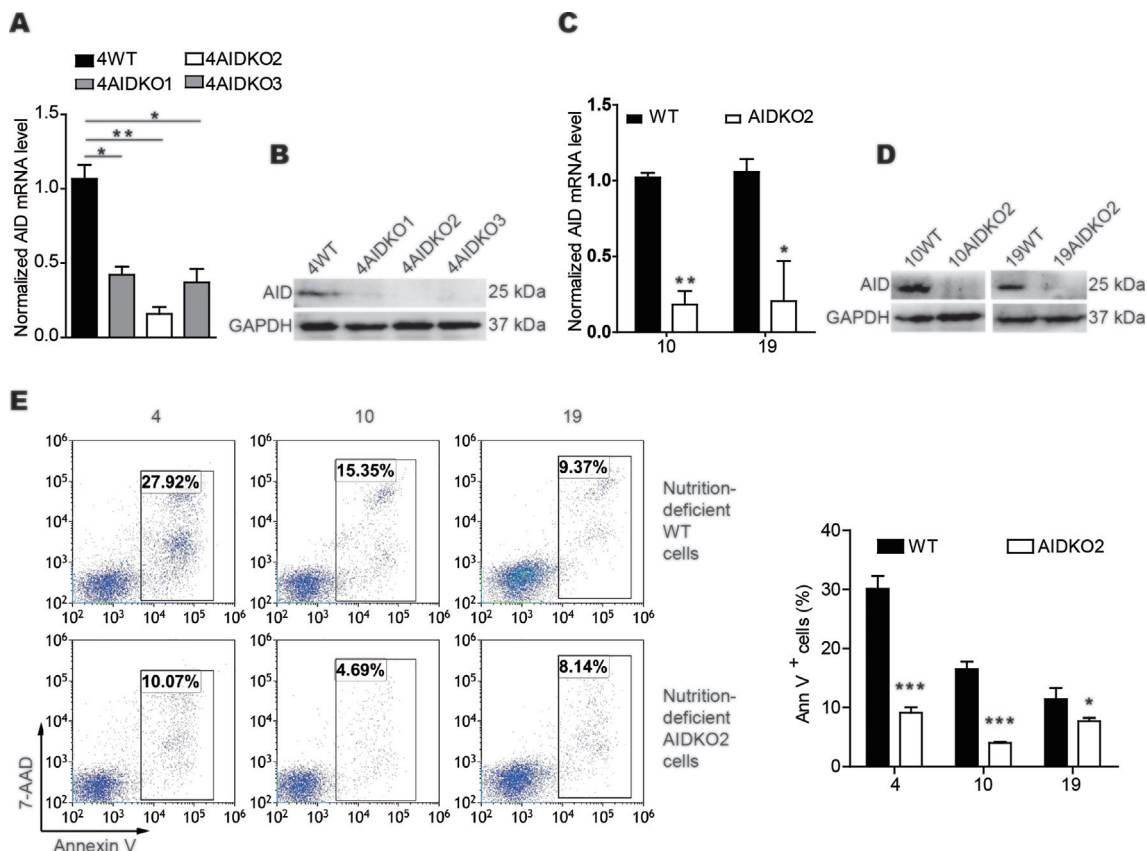

Fig. 1. AID deficiency impairs apoptosis of DLBCL cells. (A, B) *AID* depletion by three guide RNAs (AIDKO1-AIDKO3) of CRISPR/Cas9 in SU-DHL-4 cells was confirmed by qRT-PCR (A) and immunoblots (B). Data shown are representative of 3 technical replicates. GAPDH protein was used as an internal control for immunoblots. AIDKO2 was the gRNA with the best efficiency in *AICDA* knock out. SU-DHL-4 cells were represented by 4 in abbreviations. (C, D) The depleting efficiency of AID by CRISPR/Cas9 vector with AIDKO2 gRNA was also confirmed in OCI-LY10 and OCI-LY19 cells by qRT-PCR (C) and immunoblot (D). Data shown are representative of 3 technical replicates. GAPDH protein was used as an internal control. OCI-LY10 and OCI-LY19 cells were represented by 10 and 19 in abbreviations, respectively. (E) Flow cytometry was performed for apoptosis maker Annexin V and 7-AAD stained WT and AIDKO DLBCL cells (4, 10 and 19) after nutrition deficiency treatment. Histograms indicate the percentages of apoptosis cells. Data shown are representative of 3 independent experiments. Data are represented as mean þ SD. *,** and *** represent $p < 0.05$, $p < 0.01$ and $p < 0.001$, respectively.

Taken together, these results suggest that AID deficiency impairs the DLBCL cell proliferation.

To investigate whether AID was involved in *BCL6* expression in the DLBCL cells, the mRNA and protein levels of BCL6 were analyzed in WT and AIDKO DLBCL cells, respectively. We observed that the expression levels of *BCL6* increased 5 to 15 folds in AIDKO cells in comparison to that in WT cells (Fig. 2A). The specific elevated BCL6 level in three AIDKO DLBCL cells was confirmed by immunoblots (Fig. 2B). The data suggest that AID deficiency potentiates to up-regulate oncogenic BCL6 expression in DLBCL cells with higher proliferative rate.

The deamination of AID has no role for DNA demethylation on BCL6 gene

To evaluate whether AID deamination contributed to *BCL6* expression by mutations, genomic DNA was purified from WT and AIDKO DLBCL cells, respectively. It has been reported that þ1-kilobase (kb) segment of the major transcription start site (TSS) for each gene is the preferred region for AID targeting [19]. A 0.92 kb *BCL6* segment, located upstream of TSS, was selected to amplify, sequenced and analyzed for point mutations with 34 960 nucleotides of sequence (Fig. 2C). The mutation frequency for
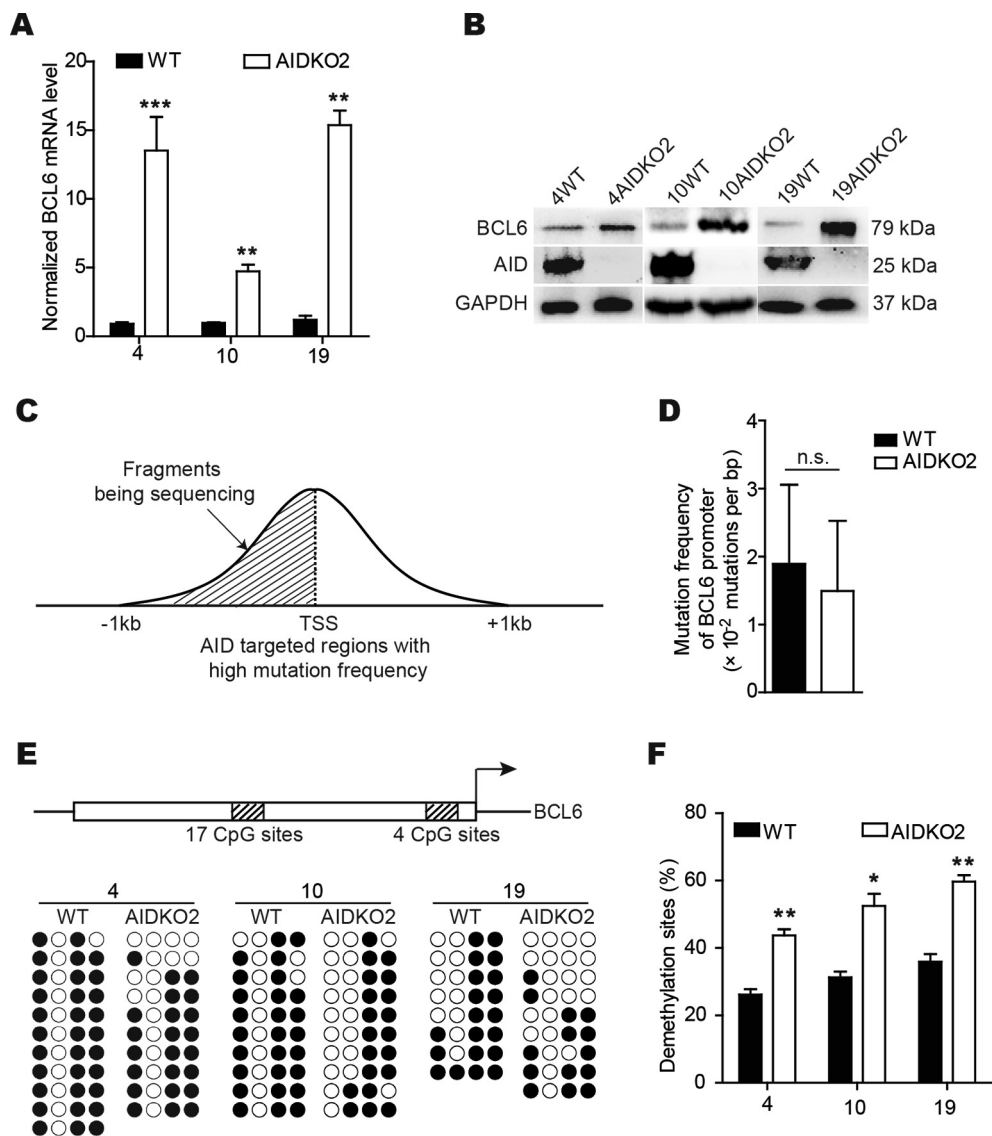

Fig. 2. The deamination of AID has no role for DNA demethylation on *BCL6* gene. (A) *BCL6* transcripts were detected in 4WT and 4AIDKO, 10WT and 10AIDKO, 19WT and 19AIDKO by qRT-PCR. Data shown are representative of 3 technical replicates. (B) BCL6 protein levels were measured in 4WT and 4AIDKO, 10AIDKO and 19AIDKO cells by immunoblots, and GAPDH protein was taken as an internal control. (C) Schematic diagram shows AID mediated *BCL6* mutation region. Not drawn to scale. (D) Histograms represent point mutation frequency of *BCL6* promoter in 4WT and 4AIDKO cells. Mutation was measured in DNA from 2 independent preparations. (E) Schematic diagram shows CpG sites in the promoter of *BCL6* gene. The hollow box represents *BCL6* promoter. The shadow boxes represent CpG sites. The segment for 17 CpG sites locates in −1.07 kb to −0.84 kb of *BCL6* promoter. The segment for 4 CpG sites is in the −0.51 kb to −0.24 kb of *BCL6* promoter. Not drawn to scale. The bisulfite sequencing was used to examine methylation status of these CpG sites in *BCL6* promoter. Black circles signify methylated CpGs, and white circles indicate demethylated CpGs. (F) Histograms indicate results for demethylation frequency of CpG sites in *BCL6* promoter as detecting in E. Methylation was measured in DNA from 2 independent preparations. Data are presented as mean þ SD. *,** and *** represent p < 0.05, p < 0.01 and p < 0.001, respectively. n.s. indicates no significance.

BCL6 analyzed from WT cells displayed 1.9×10^{-2} mutations per base pair (bp). AIDKO cells yielded about 1.34×10^{-2} mutations per bp (Fig. 2D). Comparing to the data, we conclude that *BCL6* mutation frequency shows insignificant difference between WT cells and AIDKO cells

AID involves in DNA demethylation process and usually targets promoters in B or non-B cells [5,10]. To verify the epigenetic role of AID related to *BCL6* expression in AIDKO cells, the bisulfite sequencing was used to examine methylation status of *BCL6* promoter region (Fig. 2E). The methylation level of the 4 CpG sites located in the −0.51 kb to −0.24 kb did not increase along with AID deficiency. Instead, it slightly decreased in AID-deficient DLBCL cells (Fig. 2F). However, the methylated levels of 17 CpG sites located in the −1.07 kb to −0.84 kb did not show significant difference in SU-DHL-4 cells with or without AID expression (Fig. S3A and B), suggesting an indirect role of AID in methylation on CpG sites closed to TSS in *BCL6* promoter. There is no tight link between AID deamination activity and *BCL6* demethylation.

AID assists DNMT1 to attenuate BCL6 expression via maintaining DNA methylation

To search the factors assisted by AID involved in *BCL6* methylation, we focused on conserved DNA methyltransferases, including DNMT1, DNMT3A and DNMT3B, which play the most important roles in de novo synthesis and maintenance of DNA methylation in mammal cells [32–34]. To gain more insights into the mechanism of DNA methylation controlling *BCL6* expression in DLBCL cells, we demonstrated that DNMT1 but not DNMT3A or DNMT3B dramatically reduced in AIDKO DLBCL cells compared to WT counterparts (Fig. 3A and B; Fig. S4A). To identify the involvement of endogenous DNMT1 in BCL6 methylation, we created *DNMT1* knockout SU-DHL-4 (4DNMT1KO), OCI-LY10 (10DNMT1KO) and OCI-LY19 (19DNMT1KO) cell lines using CRISPR/Cas9 technique (Fig. 3C and D; Fig. S4B). The *BCL6* expression was up-regulated in contrast to decreased DNMT1 level in the three DNMT1KO DLBCL cells (Fig. 3C and D; Fig. S4C). To test whether AID synergized DNMT1 to inhibit *BCL6* expression, 4WT and 4AIDKO DLBCL cells were treated with a DNMT1 inhibitor 5-Azacytidine [35], we showed that BCL6 mRNA level was at the peak following the repression by both AID and DNMT1 (Fig. 3E). The immunoblot analysis also confirmed a promoting effect to *BCL6* expression when both AID and DNMT1 were absent in DLBCL cells (Fig. 3F, lane 4, 8 12). These findings demonstrate that AID and DNMT1 collaborate to inhibit *BCL6* expression in DLBCL cells.

Following the revelation of a reduced DNMT1 level in AIDKO cells (Fig. 3A), we hypothesized that AID regulated DNMT1 expression at either a transcription or a post-transcription level. The transcripts of DNMT1 exhibited unconspicuous change in three DLBCL cells in presence or absence of AID (Fig. 3G), arguing that AID modulated DNMT1 expression at a post-transcription level. We used the proteasome inhibitor, MG132, which is used to inhibit protein degradation. The AID and DNMT1 expression increased in the three DLBCL cells after MG132 treatment (Fig. 3H, lane 3, 7 and 11). Meanwhile, both AID and DNMT1 were disappeared following 5-Azacytidine treatment in DLBCL cells (Fig. 3H, lane 2, 6 and 10). However, the 5-Azacytidine induced depletion was rescued by MG132 treatment (Fig. 3H, lane 4, 8 and 12). We interpreted these findings that AID and DNMT1 stabilized each other to avoid their degradation. To confirm the existence of AID-DNMT1 complex in DLBCL cells, we performed immunoprecipitation (IP) experiments to reveal the association of AID and DNMT1. Pre-clearing of nuclear extracts using anti-AID or anti-DNMT1 removed the complexes without AID or DNMT1. The complexes hosted by anti-

AID showed the existence of DNMT1 (Fig. 3I). The DNMT1-containing complexes hosted by anti-DNMT1 revealed AID existence (Fig. 3J). The results suggest that AID and DNMT1 co-reside in DLBCL cells to form complexes. Taken together, the data demonstrate that AID assists DNMT1 as a cofactor to attenuate BCL6 by maintaining DNA methylation.

AID-DNMT1 complex binds to −0.4 kb to 0 kb BCL6 promoter region

To investigate whether AID and DNMT1 bound to *BCL6* promoter directly, Chromatin Immunoprecipitation (ChIP) assays were performed using antibodies against AID and DNMT1. Immunoprecipitated DNA was analyzed by qPCR with primers that amplify two fragments which locate in −0.43 kb – −0.23 kb (site 1) and −0.21 kb – −0.03 kb (site 2) regions (Figure S5A). AID and DNMT1 binding to the two sites were extremely higher in SU-DHL-4, OCI-LY10 and OCI-LY19 cells than that in their KO counterparts, respectively (both $p < 0.05$) (Fig. 4A and B). We additionally revealed that enrichment of H3K4me3, which marked active promoter, largely presented in both WT and AIDKO cells (Figure S5B), suggesting that AID-DNMT1 complex binds to H3k4me3 enriched *BCL6* promoter directly.

To identify whether the distinct recruitment of AID contributed to the repression of *BCL6* transcription, a 1.8 kb *BCL6* promoter segment (p) (positions −1.8 kb to −0 kb) was amplified and ligated to constructs with a firefly luciferase–encoding region (Fig. 4C). We observed that the construct with p induced more than 3 folds higher relative luciferase activity in AIDKO DLBCL cells than that in WT DLBCL cells ($p < 0.05$) (Fig. 4D to F), indicating AID loss induced *BCL6* promoter-driven transcription initiation. To further test the potential AID targeted minimum sequence needed for repressing *BCL6* transcription, we generated four luciferase reporter assay systems containing four small segments derived from the 1.8 kb region, including p1 (positions −0.4 kb to 0 kb), p2 (positions −0.9 kb to −0.4 kb), p3 (positions −1.4 kb to −0.9 kb) and p4 (positions −1.8 kb to −1.4 kb) (Fig. 4C). The construct with p1 induced approximately 2.5 to 3 folds more relative luciferase activity in AIDKO DLBCL cells than that in WT DLBCL cells (all $p < 0.05$), while other three segments (p2, p3 and p4) had no function in arousing luciferase activity (Fig. 4D to F), suggesting p1 was the specific region that AID functionally repressed *BCL6* expression. Similarly, we tested p and p1 regions mediated nearly 3 to 5 folds more relative luciferase activity in DNMT1KO cells than WT cells (Fig. 4G to I), indicating the minimal sequence of AID and DNMT1 targeting is −0.4 kb to 0 kb in *BCL6* promoter. Together, these results suggest AID-DNMT1 complex abrogates *BCL6* transcription level by binding to the −0.4 kb −0 kb region of *BCL6* promoter in DLBCL cells.

MG132 suppresses DLBCL growth in vitro and in vivo

On the basis that AID-DNMT1 complex inhibited *BCL6* transcription in DLBCL cells, we asked whether MG132 suppressed transcription level of *BCL6* was capable of antilymphoma activity in DLBCL. After the treatment of WT, AIDKO2 and DNMT1KO3 cells derived from SU-DHL-4, OCI-LY10 and OCI-LY19 cell lines with MG132, the trend of cell apoptosis was observed by analyzing Annexin V staining. The apoptosis ratios of MG132 treated WT, AIDKO2 and DNMT1KO3 DLBCL cells apparently increased (Fig. 5A). The cytotoxicity of MG132 to WT DLBCL cells were superior to either AIDKO2 or DNMT1KO3 cells, indicating that MG132 killing DLBCL cells through accumulating AID and DNMT1 (Fig. 5A). The active caspase 3 level rose after MG132 treatment (Fig. S6A). In addition, the anti-apoptotic gene expression including *BCL6* as well as *BCL2* also dropped ($p < 0.05$) (Fig. S6B). Several apopto-
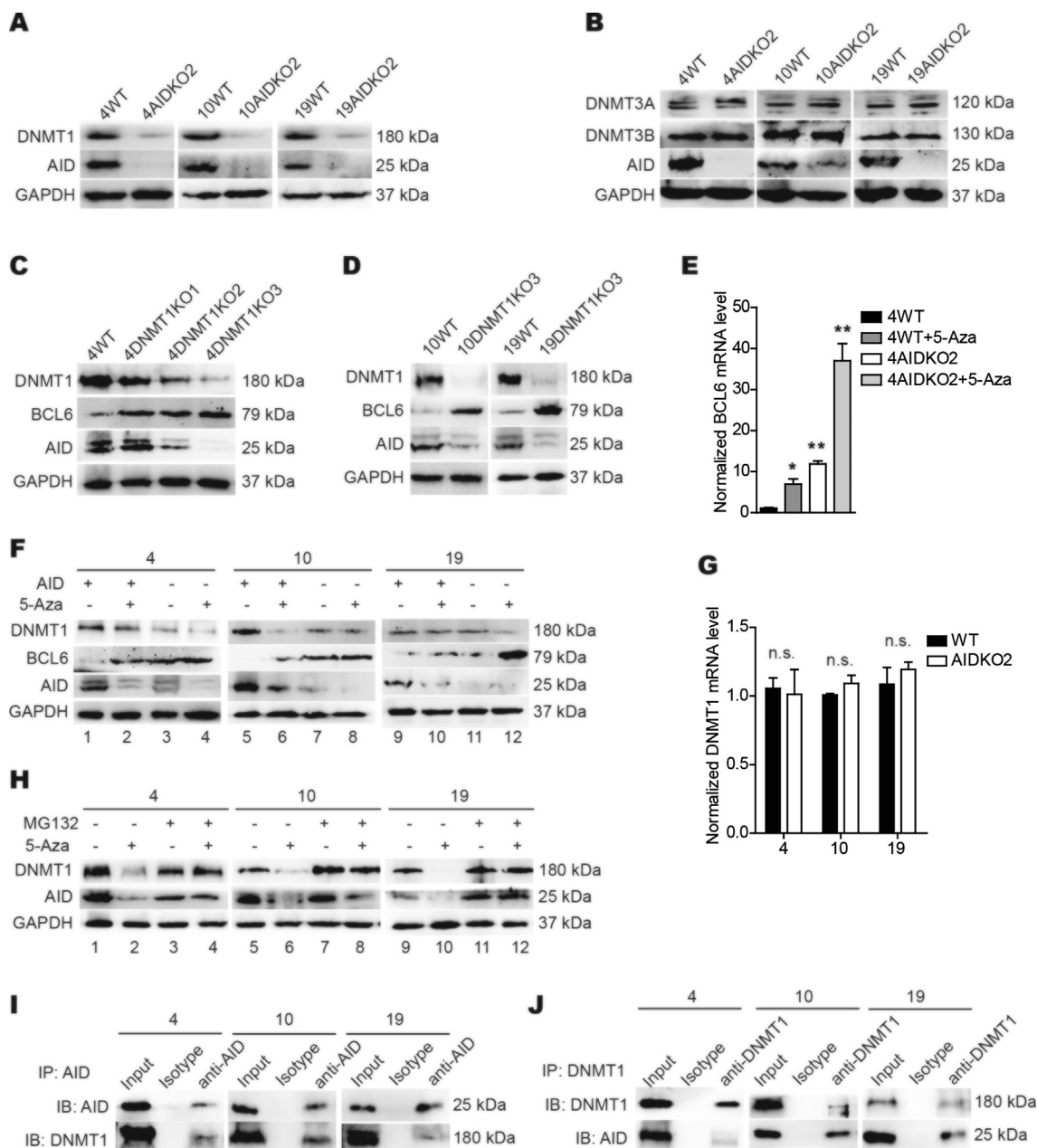
Fig. 3. The stabilized AID-DNMT1 complex suppresses *BCL6* expression in DLBCL cells. (A) Immunoblot measurement of DNMT1 and AID protein level was performed in 4WT and 4AIDKO, 10WT and 10AIDKO, 19WT and 19AIDKO cells, respectively. GAPDH protein was used as an internal control. (B) DNMT3A, DNMT3B and AID proteins were measured in WT and AIDKO DLBCL cells by immunoblots. GAPDH protein was taken as an internal control. (C) Immunoblot detection of DNMT1, AID and BCL6 proteins was performed in SU-DHL-4 cells with CRISPR/Cas9 including three gRNAs for depleting DNMT1. DNMT1KO3 was the gRNA with the best efficiency in *DNMT1* knock out. GAPDH protein was used as an internal control. (D) DNMT1, AID and BCL6 protein levels were detected in 10WT, 19WT and 10DNMT1KO, 19DNMT1KO cells by immunoblots, and GAPDH protein was used as an internal control. (E) *BCL6* transcripts were detected in 4WT and 4AIDKO cells after 5-Azacytidine (10 μM) (5-Aza) treatment for 24 hours *in vitro* by qRT-PCR. Data shown are representative of 3 technical replicates. (F) DNMT1, BCL6 and AID protein levels were detected in 4WT and 4AIDKO, 10WT and 10AIDKO, 19WT and 19AIDKO cells treated with 5-Azacytidine as in E. GAPDH protein was used as an internal control. (G) DNMT1 transcripts were detected in 4WT and 4AIDKO, 10WT and 10AIDKO, 19WT and 19AIDKO cells by qRT-PCR. Data shown are representative of 3 technical replicates. (H) Immunoblots of DNMT1 and AID protein levels were performed in 4, 10 and 19 cells treated with MG132 (10 μM) and/or 5-Azacytidine (10 μM). GAPDH protein was taken as an internal control. The 5-Azacytidine treatment was 24 hours, and MG132 treatment was 8 hours, the combined treatment of DLBCL cells (4, 10 and 19) was performed by adding MG132 following 5-Azacytidine treatment for 16 hours to continuously treat for 8 hours. (I, J) DNMT1 and AID proteins were detected by immunoblots after immunoprecipitation (IP) by anti-AID pulldown (I) and anti-DNMT1 (J) in 4, 10 and 19 cells. Data shown are representative of 3 independent experiments. Data are presented as mean þ SD. *,** and *** represent p < 0.05, p < 0.01 and p < 0.001, respectively. n.s. indicates no significance.
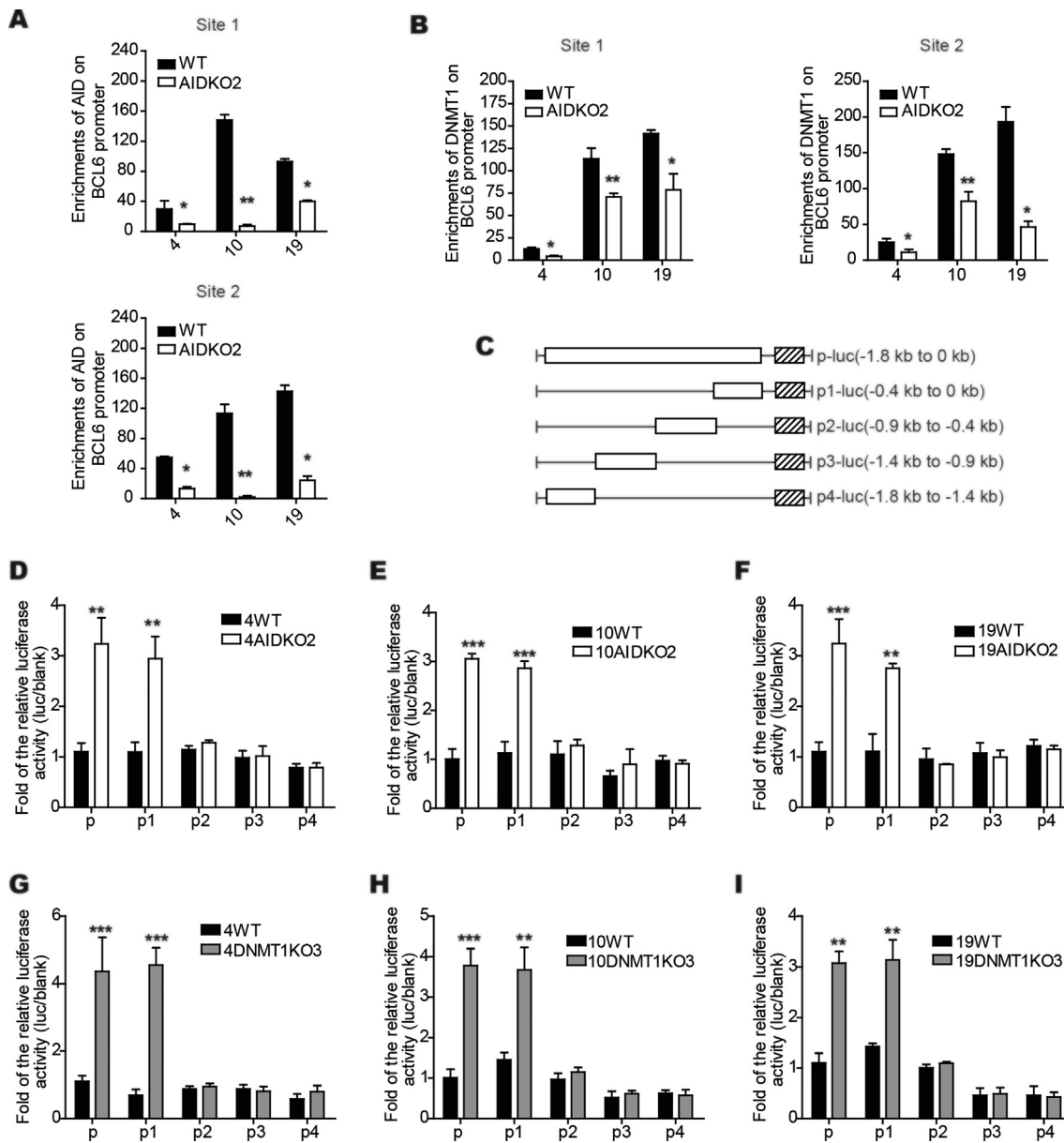
Fig. 4. AID-DNMT1 complex binds to *BCL6* promoter. (A, B) Enrichments of AID binding (A) and DNMT1 binding (B) to the two sites of *BCL6* promoter in 4WT and 4AIDKO, 10WT and 10AIDKO, 19WT and 19AIDKO cells, respectively. Chromatin Immunoprecipitation (ChIP) was performed using anti-AID and anti-DNMT1 following quantitative PCR amplifying two binding sites from ChIP enriched DNA. Data were collected from 3 independent experiments. Data shown are representative of 3 technical replicates. (C) Schematic diagram shows the indicated regions amplified from the *BCL6* promoter to prepare the constructs for luciferase activity assay, the hollow boxes indicates the amplified fragments, shadow boxes represents pGL3-basic elements. p, a 1.8 kb *BCL6* promoter (positions −1.8 kb to 0 kb); p1, p2, p3, p4 represents 0.4 kb (positions −0.4 kb to 0 kb), 0.5 kb (positions −0.9 kb to −0.4 kb), 0.5 kb (positions −1.4 kb to −0.9 kb), 0.4 kb (positions −1.8 kb to −1.4 kb) regions in *BCL6* promoter. (D, E, F) Luciferase activity in 4WT and 4AIDKO (D), 10WT and 10AIDKO (E), 19WT and 19AIDKO (F) cells transfected with PGL3-basic vector including the indicated BC*L6* promoter fragments was detected, the results were shown as histograms. Data shown are representative of 3 independent experiments. (G, H, I) Luciferase activity assay of PGL3-basic vector with the indicated *BCL6* promoter fragments in 4WT and 4DNMT1KO (G), 10WT and 10DNMT1KO (H), 19WT and 19DNMT1KO (I) cells was performed, the results were shown as histograms. Data shown are representative of 3 independent experiments. Data are represented as mean þ SD. *,** and *** represent p < 0.05, p < 0.01 and p < 0.001, respectively. n.s. indicates no significance.

sis associated genes (for example, *BIMEI*, *BMF*, *BOK*, *BAD*, *PUMA*, *BAK*) level apparently increased (all p < 0.05) (Fig. S6C). In general, MG132 has the ability to induce DLBCL cell apoptosis by inhibiting DNMT1 and AID degradation through proteasome pathway.

To determine whether MG132 could affect lymphoma growth *in vivo*, the murine WT, AIDKO2 and DNMT1KO3 DLBCL cells xenogeneic

tumor model were generated. When the tumor volume reached to 80 mm³–100 mm³, the intraperitoneal administration of solvent or MG132 to mice was performed (Fig. S6D). The administration of MG132 strongly impaired the expansion of WT DLBCL cells, manifesting reduced tumor volume and tumor weight. In contrast, solvent treatment completely failed to exert any inhibitory effects on the progression
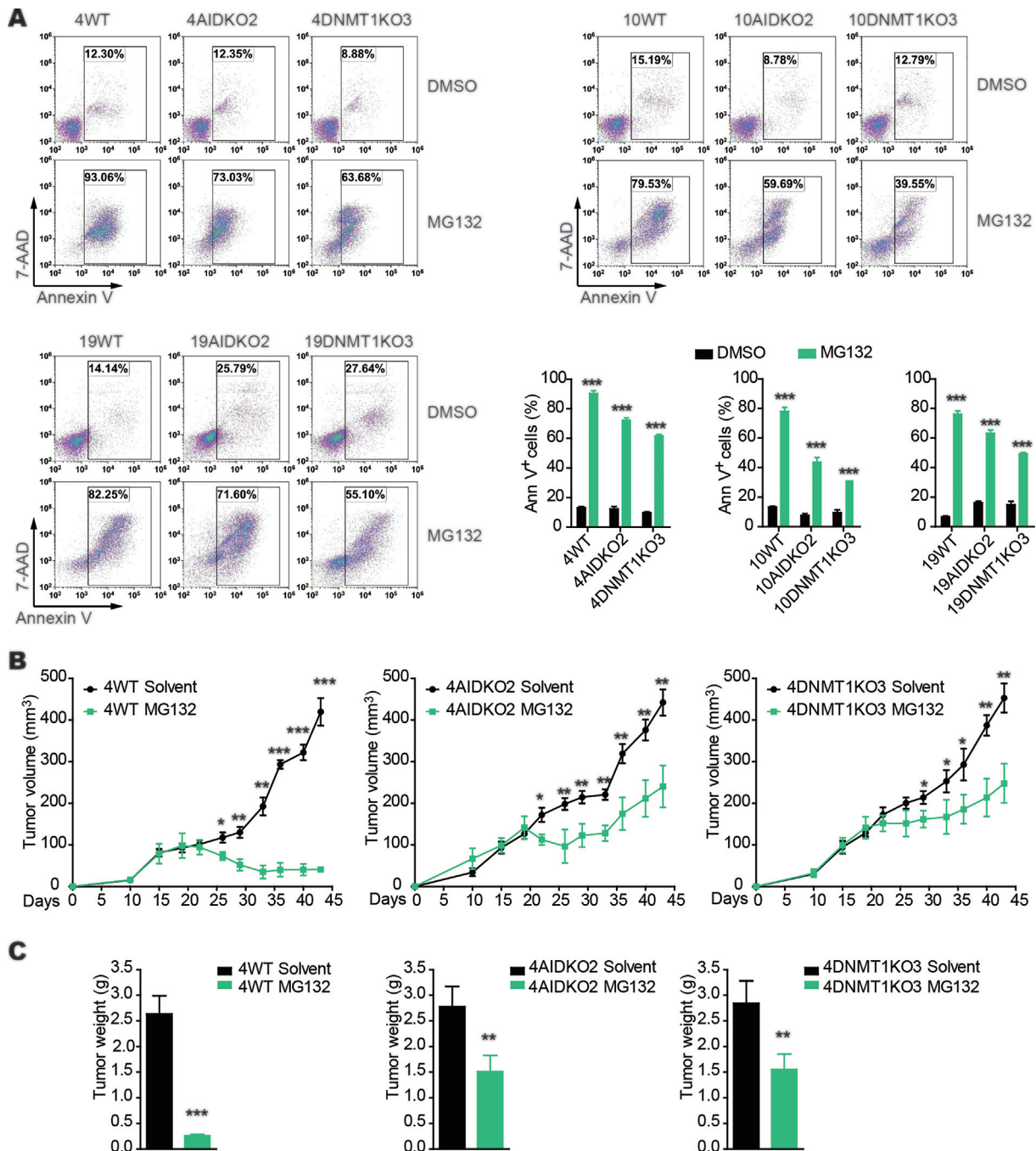
Fig. 5. MG132 inhibits DLBCL cell growth *in vitro* and *in vivo*. (A) Flow cytometry was used to detected the apoptotic marker Annexin V and 7-AAD stained WT, AIDKO2 and DNMT1KO3 DLBCL cells treated with DMSO or MG132 treatment (10 μM) for 8 hours. The dot plot indicated the cell population undergoing apoptosis; histograms show the percentages of population for apoptosis cells. Data shown are representative of 3 independent experiments. (B) Histograms indicate results of 4WT, 4AIDKO2 and 4DNMT1KO3 cells xenogeneic tumor volumes monitored through the whole tumorigenesis and treatment (n = 5). (C) Histograms show the data for 4WT, 4AIDKO2 and 4DNMT1KO3 cells xenogeneic tumor weight measurement following tumor excision from the sacrificed mice (n = 5). Data are represented as mean þ SD. *** represent p < 0.001.

of WT DLBCL cells, showing big tumor volume and much tumor weight (Fig. 5B and C). However, the tumor volume and tumor weight from AIDKO2 and DNMT1KO3 cells xenogeneic tumor models showed relatively inefficient inhibition effect after MG132 treatment, indicating that MG132 inhibited DLBCL xenogeneic tumor growth via increasing AID and DNMT1 activity at the BCL6 promoter region *in vivo*. These findings indicate that MG132 has a significant therapy function in the treatment of DLBCL disease *in vitro* and *in vivo*.

Discussion

Many experiments in a variety of systems have confirmed the role of AID in plastic diversity of DNA methylation and corresponding gene regulation in normal GCBs. DLBCLs originate from GCBs and are characterized by BCL6 dysregulation [5,11,36]. However, until now, the connections are limited between AID's epigenetic role or cofactor role and *BCL6* expression in DLBCL. The present results here demonstrate

that AID assists DNMT1 to bind to −0.4 kb −0 kb segment of *BCL6* promoter and mediates BCL6 to undergo DNA methylation. The process consequently inhibits BCL6 expression in DLBCLs without *BCL6* mutations or translocations, thereby providing a mechanism for the therapy of proteasome inhibitor MG132 to DLBCL by inducing accumulation of AID and DNMT1. The data here reveal that an alternative cofactor role of AID to DNMT1 in maintaining BCL6 methylation in DLBCL.

Deregulated BCL6 expression is commonly associated with DLBCLs, due to its promoter mutations, chromosomal translocations or epigenetic modifications or cofactor role in gene expression [22,37,38]. Therefore, understanding BCL6 deregulation from AID mediated gene expression regulation by epigenetic alteration or alternative cofactor role could help in revealing molecular pathogenesis of DLBCLs beyond AID associated mutations or translocations [27]. Studies on AID targeting in the genome have been demonstrated that AID occupies at a large number of promoters beyond Ig loci, implying AID might be involved in controlling gene expression [39]. Here, we show that AID and DNMT1 formed complex to bind to *BCL6* promoter (Fig. 3 and Fig. 4). This indicates that the occupancy of AID-DNMT1 complex on *BCL6* promoter efficiently impedes the access of transcription initiation factors to *BCL6* locus, thus suppresses *BCL6* transcription in DLBCL. Notably, the data provided here indicate that the methylated CpG sites (−0.51 kb to −0.24 kb) are located in the AID-DNMT1 complex binding region in BCL6 promoter (−0.4 kb −0 kb) (Fig. 2 and Fig. 4). On the basis of our findings and those of others [33], we suggest that DNMT1 instead of AID is a key factor to maintain methylation of *BCL6* promoter in DLBCL (Fig. 2, Fig. 5 and Fig. S3). AID recruits DNMT1 to the −0.4 kb −0 kb region of *BCL6* and assists DNMT1 as a cofactor to maintain the methylation of *BCL6* promoter, thus represses *BCL6* expression in DLBCL.

The role of AID to *BCL6* in DLBCL is depicted as AID mediated *BCL6* mutations or translocations inducing uncontrolled *BCL6* expression [27,37–39]. We excluded structural variants of *BCL6* locus in the DLBCL cells used in our experiments (Fig. 2). Our results demonstrate that AID assisted DNMT1 to inhibit *BCL6* transcription through maintaining DNA methylation on its promoter (Fig. 3, Fig. 4 and Fig. S3). It seems that one contradiction between the common deamination function of AID to *BCL6* and our results appeared. One likely explanation for this is that the reported high expression of AID in DLBCL is the effect of its antagonism to *BCL6* high expression. Our hypothesis was confirmed by constructing *BCL6* and *AID* over-expressing DLBCL cell lines. The data indicate that overexpressed *BCL6* increases *AID* levels (Fig. S7A and B), while increased *AID* forces to reduce *BCL6* expression (Fig. S7C and Fig. 2).

For the initiator of DLBCL pathogenesis, we propose that AID off-target might be the main driver of DLBCL with *BCL6* translocations, while BCL6 deregulation may be the main inducer of DLBCL without *BCL6* translocations. It seems that AID has two edges in DLBCL. For DLBCL without translocations, up-regulation of AID might be a positive way to perform antagonism to BCL6 induced DLBCL deterioration. Therefore, we suggest a AID-BCL6 regulation loop in DLBCL. Firstly, BCL6 deregulation drives the deterioration of DLBCL, high expression of BCL6 mediate up-regulation of AID. Secondly, to antagonize BCL6 driven DLBCL, highly expressed AID consecutively down-regulates *BCL6* level through forming complex with DNMT1 (Fig. S7D).

In the last decade, many novel therapeutic regimens have been developed to treat DLBCL, such as radio- and/or immuno-, multi-agent chemotherapy, and even R-CHOP [40–43]. Clinical therapeutic strategies for DLBCL by targeting *BCL6* through BCL6 inhibition or degradation are well appreciated [44–47]. However, these conventional therapeutic methods have less mitigation effect in cancer therapy, there are still more than 30% of patients, who are non-responsive to the available treatment or will develop relapsed/refractory disease with resistance [48]. Based on the

data shown here, we attempted to find another effective therapeutic approach for DLBCL. Therefore, a proteasome inhibitor, MG132, was used here to treat DLBCL. Indeed, it is found from the treatment data *in vitro* and *in vivo* that AID and DNMT1 accumulation by MG132 treatment can slow down the disease progression or even treat DLBCL (Fig. 5), suggesting a new selective therapy strategy in clinical DLBCL treatment. The MG132 treatment suppressed *BCL6* transcription in DLBCL, which is superior to and eliminated the post-transcription degradation of BCL6 protein.

Here, our data support a possible model by which the interaction of AID and DNMT1 controls *BCL6* transcription in DLBCL: (1) the loss of AID or DNMT1 leads AID-DNMT1 complex to disassociate from *BCL6* promoter. As a consequence, the methylated *BCL6* promoter undergoes demethylation and the expression of *BCL6* increases in DLBCL (Fig. 6A). (2) AID-DNMT1 complex is recruited to the −0.4 kb −0 kb region of *BCL6* promoter, AID assists DNMT1 to maintain methylation of *BCL6* promoter and inhibits *BCL6* expression in DLBCL (Fig. 6B). (3)
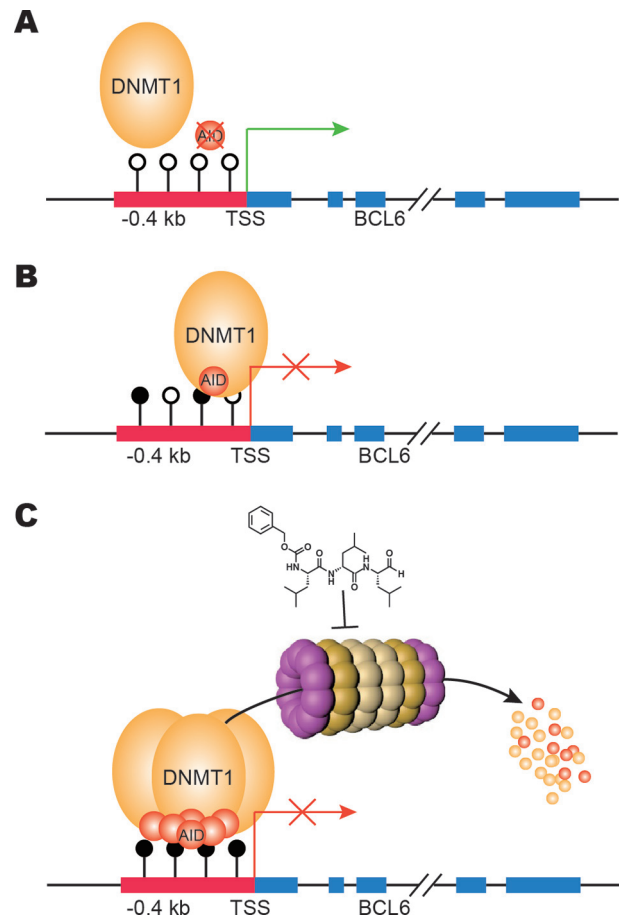

Fig. 6. Model for AID-DNMT1 complex suppressing BCL6 expression in DLBCL. (A) Loss of AID or DNMT1 causes instability of AID-DNMT1 complex. The disassociation of AID-DNMT1 from *BCL6* promoter induces demethylation of *BCL6* promoter, thus induces increased BCL6 expression in DLBCL. (B) AID-DNMT1 complex binds to the −0.4 kb −0 kb region of *BCL6* promoter, their cooperation maintains methylation of *BCL6* promoter and inhibits *BCL6* expression in DLBCL. (C) MG132 treatment stabilizes AID-DNMT1 complex to bind to *BCL6* promoter, drives dynamic methylation of *BCL6* promoter and down regulates *BCL6*, which shows a treatment of MG132 to BCL6-driven DLBCL.

MG132 mediates *BCL6* repression by avoiding AID and DNMT1 degradation. AID-DNMT1 complex has more opportunity to be recruited to *BCL6* promoter, and drives dynamic methylation (Fig. 6C).

In conclusion, our work provides a novel mechanism of AID and DNMT1 cooperation maintains the methylation of *BCL6* promoter, which in turn suppresses *BCL6* expression in DLBCL. Our model might be useful for clinical staging of DLBCL by using AID and BCL6 proteins. In addition, blockade of AID and DNMT1 degradation by proteasome inhibitor MG132 could induce DLBCL cell apoptosis and would develop an effective therapeutic strategy for DLBCL in future.

Acknowledgements

Conflict of Interest

The authors do not have any conflict of interest.

Data and materials availability

All data needed to evaluate the conclusions in the paper are present in the paper or in the Supplementary Materials.

Appendix A. Supplementary data

Supplementary data to this article can be found online at https://doi.org/10.1016/j.neo.2020.01.002.

References

1. Muramatsu M, Kinoshita K, Fagarasan S, Yamada S, Shinkai Y, Honjo T. Class switch recombination and hypermutation require activation-induced cytidine deaminase (AID), a potential RNA editing enzyme. *Cell* 2000;**102**:553–63.
2. Leeman-Neill RJ, Lim J, Basu U. The common key to class-switch recombination and somatic hypermutation: discovery of AID and its role in antibody gene diversification. *J Immunol* 2018;**201**:2527–9.
3. Murre C. A common mechanism that underpins antibody diversification. *Cell* 2015;**163**:1055–6.
4. Ersching J, Efeyan A, Mesin L, Jacobsen JT, Pasqual G, Grabiner BC, Dominguez-Sola D, Sabatini DM, Victora GD. Germinal Center Selection and Affinity Maturation Require Dynamic Regulation of mTORC1 Kinase. *Immunity* 2017;**46**:1045–58, e1046.
5. Teater M, Dominguez PM, Redmond D, Chen Z, Ennishi D, Scott DW, Cimmino L, Ghione P, Chaudhuri J, Gascoyne RD, et al. AICDA drives epigenetic heterogeneity and accelerates germinal center-derived lymphomagenesis. *Nat Commun* 2018;**9**:222.
6. Crouch EE, Li Z, Takizawa M, Fichtner-Feigl S, Gourzi P, Montano C, Feigenbaum L, Wilson P, Janz S, Papavasiliou FN, et al. Regulation of AID expression in the immune response. *J Exp Med* 2007;**204**:1145–56.
7. Qiao Q, Wang L, Meng FL, Hwang JK, Alt FW, Wu H. AID recognizes structured DNA for class switch recombination. *Mol Cell* 2017;**67**(361–373) e364.
8. Dong J, Panchakshari RA, Zhang T, Zhang Y, Hu J, Volpi SA, Meyers RM, Ho YJ, Du Z, Robbiani DF, et al. Orientation-specific joining of AID-initiated DNA breaks promotes antibody class switching. *Nature* 2015;**525**:134–9.
9. Pham P, Afif SA, Shimoda M, Maeda K, Sakaguchi N, Pedersen LC, Goodman MF. Activation-induced deoxycytidine deaminase: Structural basis for favoring WRC hot motif specificities unique among APOBEC family members. *DNA Repair (Amst)* 2017;**54**:8–12.
10. Dominguez PM, Teater M, Chambwe N, Kormaksson M, Redmond D, Ishii B, Vuong B, Chaudhuri J, Melnick A, Vasanthakumar A, et al. DNA methylation dynamics of germinal center B cells are mediated by AID. *Cell Rep* 2015;**12**:2086–98.
11. Wang Q, Oliveira T, Jankovic M, Silva IT, Hakim O, Yao K, Gazumyan A, Mayer CT, Pavri R, Casellas R, et al. Epigenetic targeting of activation-induced cytidine deaminase. *Proc Natl Acad Sci USA* 2014;**111**:18667–72.
12. Dominguez PM, Shaknovich R. Epigenetic function of activation-induced cytidine deaminase and its link to lymphomagenesis. *Front Immunol* 2014;**5**:642
13. Ramiro AR, Barreto VM. Activation-induced cytidine deaminase and active DNA demethylation. *Trends Biochem Sci* 2015;**40**:172–81.
14. Schuermann D, Weber AR, Schar P. Active DNA demethylation by DNA repair: Facts and uncertainties. *DNA Repair (Amst)* 2016;**44**:92–102.
15. Pavri R, Gazumyan A, Jankovic M, Di Virgilio M, Klein I, Ansarah-Sobrinho W, Resch W, Yamane A, Reina San-Martin B, Barreto V, et al. Activation-induced cytidine deaminase targets DNA at sites of RNA polymerase II stalling by interaction with Spt5. *Cell* 2010;**143**:122–33.
16. Methot SP, Litzler LC, Subramani PG, Eranki AK, Fifield H, Patenaude AM, Gilmore JC, Santiago GE, Bagci H, Cote JF, et al. A licensing step links AID to transcription elongation for mutagenesis in B cells. *Nature Commun* 2018;**9**:1248
17. Pham P, Malik S, Mak C, Calabrese PC, Roeder RG, Goodman MF. AID-RNA polymerase II transcription-dependent deamination of IgV DNA. *Nucleic Acids Res* 2019.
18. Duke JL, Liu M, Yaari G, Khalil AM, Tomayko MM, Shlomchik MJ, Schatz SH, Kleinstein SH. Multiple transcription factor binding sites predict AID targeting in non-Ig genes. *J Immunol* 2013;**190**:3878–88.
19. Liu M, Duke JL, Richter DJ, Vinuesa CG, Goodnow CC, Kleinstein SH, Schatz DG. Two levels of protection for the B cell genome during somatic hypermutation. *Nature* 2008;**451**:841–5.
20. Hatzi K, Geng H, Doane AS, Meydan C, LaRiviere R, Cardenas M, Duy C, Shen H, Vidal MNC, Baslan T, et al. Histone demethylase LSD1 is required for germinal center formation and BCL6-driven lymphomagenesis. *Nat Immunol* 2019;**20**:86–96.
21. Bunting KL, Melnick AM. New effector functions and regulatory mechanisms of BCL6 in normal and malignant lymphocytes. *Curr Opin Immunol* 2013;**25**:339–46.
22. Basso K, Schneider C, Shen Q, Holmes AB, Setty M, Leslie C, Dalla-Favera R. BCL6 positively regulates AID and germinal center gene expression via repression of miR-155. *J Exp Med* 2012;**209**:2455–65.
23. Zaheen A, Boulianne B, Parsa JY, Ramachandran S, Gommerman JL, Martin A. AID constrains germinal center size by rendering B cells susceptible to apoptosis. *Blood* 2009;**114**:547–54.
24. Allen CD, Ansel KM, Low C, Lesley R, Tamamura H, Fujii N, Cyster JG. Germinal center dark and light zone organization is mediated by CXCR4 and CXCR5. *Nat Immunol* 2004;**5**:943–52.
25. Tas JM, Mesin L, Pasqual G, Targ S, Jacobsen JT, Mano YM, Chen CS, Weill CA, Reynaud CA, Browne EP, et al. Visualizing antibody affinity maturation in germinal centers. *Science* 2016;**351**:1048–54.
26. Leeman-Neill RJ, Bhagat G. BCL6 as a therapeutic target for lymphoma. *Expert Opin Ther Targets* 2018;**22**:143–52.
27. Duan S, Cermak L, Pagan JK, Rossi M, Martinengo C, di Celle PF, Chapuy B, Shipp M, Chiarle R, Pagano M. FBXO11 targets BCL6 for degradation and is inactivated in diffuse large B-cell lymphomas. *Nature* 2012;**481**:90–3.
28. Ji Y, Little AJ, Banerjee JK, Hao B, Oltz EM, Krangel MS, Schatz DG. Promoters, enhancers, and transcription target RAG1 binding during V(D)J recombination. *J Exp Med* 2010;**207**:2809–16.
29. Ji Y, Resch W, Corbett E, Yamane A, Casellas R, Schatz DG. The in vivo pattern of binding of RAG1 and RAG2 to antigen receptor loci. *Cell* 2010;**141**:419–31.
30. Lu Z, Tsai AG, Akasaka T, Ohno H, Jiang Y, Melnick AM, Greisman HA, Lieber MR. BCL6 breaks occur at different AID sequence motifs in Ig-BCL6 and non-Ig-BCL6 rearrangements. *Blood* 2013;**121**:4551–4.
31. Saito M, Gao J, Basso K, Kitagawa Y, Smith PM, Bhagat G, Pernis A, Pasqualucci L, Dalla-Favera R. A signaling pathway mediating downregulation of BCL6 in germinal center B cells is blocked by BCL6 gene alterations in B cell lymphoma. *Cancer Cell* 2007;**12**:280–92.

32. Hopp L, Loffler-Wirth H, Binder H. Epigenetic Heterogeneity of B-Cell Lymphoma: DNA Methylation, gene expression and chromatin states. *Genes (Basel)* 2015;**6**:812–40.

33. Farlik M, Halbritter F, Muller F, Choudry FA, Ebert P, Klughammer J, Farrow A, Santoro A, Ciaurro V, Mathur A, et al. DNA methylation dynamics of human hematopoietic stem cell differentiation. *Cell Stem Cell* 2016;**19**:808–22

34. von Meyenn F, Iurlaro M, Habibi E, Liu NQ, Salehzadeh-Yazdi A, Santos F, Petrini E, Milagre I, Yu M, Xie Z, et al. Impairment of DNA methylation maintenance is the main cause of global demethylation in naive embryonic stem cells. *Mol Cell* 2016;**62**:983.

35. Tsai CT, Yang PM, Chern TR, Chuang SH, Lin JH, Klemm L, Muschen M, Chen CC. AID downregulation is a novel function of the DNMT inhibitor 5-aza-deoxycytidine. *Oncotarget* 2014;**5**:211–23.

36. Zhang J, Grubor V, Love CL, Banerjee A, Richards KL, Mieczkowski PA, Dunphy C, Choi W, Au WY, Srivastava G, et al. Genetic heterogeneity of diffuse large B-cell lymphoma. *Proc Natl Acad Sci USA* 2013;**110**:1398–403.

37. Basso K, Dalla-Favera R. Roles of BCL6 in normal and transformed germinal center B cells. *Immunol Rev* 2012;**247**:172–83.

38. Ci W, Polo JM, Cerchietti L, Shaknovich R, Wang L, Yang SN, Ye K, Farinha DE, Horsman DE, Gascoyne RD, et al. The BCL6 transcriptional program features repression of multiple oncogenes in primary B cells and is deregulated in DLBCL. *Blood* 2009;**113**:5536–48.

39. Qian J, Wang Q, Dose M, Pruett N, Kieffer-Kwon KR, Resch W, Liang G, Tang Z, Mathe E, Benner C, et al. B cell super-enhancers and regulatory clusters recruit AID tumorigenic activity. *Cell* 2014;**159**:1524–37.

40. Reddy A, Zhang J, Davis NS, Moffitt AB, Love CL, Waldrop A, Leppa S, Pasanen A, Meriranta L, Karjalainen-Lindsberg ML, et al. Genetic and functional drivers of diffuse large B cell lymphoma. *Cell* 2017;**171**(481–494) e415.

41. Hitz F, Connors JM, Gascoyne RD, Hoskins P, Moccia A, Savage KJ, Sehn T, Shenkier T, Villa D, Klasa R. Outcome of patients with primary refractory diffuse large B cell lymphoma after R-CHOP treatment. *Ann Hematol* 2015;**94**:1839–43.

42. Lukenbill J, Hill B. Relapsed/refractory diffuse large B-cell lymphoma: review of the management of transplant-eligible patients. *Leukemia Lymphoma* 2015;**56**:293–300.

43. Chapuy B, Stewart C, Dunford AJ, Kim J, Kamburov A, Redd RA, Lawrence MGM, Roemer MGM, Li AJ, Ziepert M, et al. Molecular subtypes of diffuse large B cell lymphoma are associated with distinct pathogenic mechanisms and outcomes. *Nat Med* 2018;**24**:679–90.

44. Parekh S, Prive G, Melnick A. Therapeutic targeting of the BCL6 oncogene for diffuse large B-cell lymphomas. *Leukemia Lymphoma* 2008;**49**:874–82.

45. Cerchietti LC, Ghetu AF, Zhu X, Da Silva GF, Zhong S, Matthews M, Bunting KL, Polo JM, Fares C, Arrowsmith CH, et al. A small-molecule inhibitor of BCL6 kills DLBCL cells in vitro and in vivo. *Cancer Cell* 2010;**17**:400–11.

46. Kerres N, Steurer S, Schlager S, Bader G, Berger H, Caligiuri M, Dank C, Engen JR, Ettmayer P, Fischerauer B, et al. Chemically induced degradation of the oncogenic transcription factor BCL6. *Cell Rep* 2017;**20**:2860–75.

47. Wagner SD, Ahearne M, Ko Ferrigno P. The role of BCL6 in lymphomas and routes to therapy. *British J Haematol* 2011;**152**:3–12.

48. Pasqualucci L, Dalla-Favera R. SnapShot: diffuse large B cell lymphoma. *Cancer Cell* 2014;**25**, 132-132 e131.